




Improved Thermal and Reusability Properties of Xylanase by Genipin Cross-Linking to Magnetic Chitosan Particles

Jorge Gracida¹ · Teresita Arredondo-Ochoa² · Blanca E. García-Almendárez² ·
Montserrat Escamilla-García¹ · Keiko Shirai³ · Carlos Regalado² · Aldo Amaro-Reyes² 

Received: 27 August 2018 / Accepted: 19 November 2018 /
Published online: 27 November 2018

© Springer Science+Business Media, LLC, part of Springer Nature 2018

Abstract

Enzymes are gradually increasingly preferred over chemical processes, but commercial enzyme applications remain limited due to their low stability and low product recovery, so the application of an immobilization technique is required for repeated use. The aims of this work were to produce stable enzyme complexes of cross-linked xylanase on magnetic chitosan, to describe some characteristics of these complexes, and to evaluate the thermal stability of the immobilized enzyme and its reusability. A xylanase was cross-linked to magnetite particles prepared by in situ co-precipitation of iron salts in a chitosan template. The effect of temperature, pH, kinetic parameters, and reusability on free and immobilized xylanase was evaluated. Magnetization, morphology, size, structural change, and thermal behavior of immobilized enzyme were described. 1.0 ± 0.1 μg of xylanase was immobilized per milligram of superparamagnetic chitosan nanoparticles via covalent bonds formed with genipin. Immobilized xylanase showed thermal, pH, and catalytic velocity improvement compared to the free enzyme and can be reused three times. Heterogeneous aggregates of 254 nm were obtained after enzyme immobilization. The immobilization protocol used in this work was successful in retaining enzyme thermal stability and could be important in using natural compounds such as Fe_3O_4 @Chitosan@Xylanase in the harsh temperature condition of relevant industries.

Keywords Xylanase · Immobilization · Cross-linking · Magnetic nanoparticles · Chitosan

✉ Aldo Amaro-Reyes
aldo.amaro@uaq.edu.mx

¹ Facultad de Química, Universidad Autónoma de Querétaro, Centro Universitario, Cerro de las Campanas s/n Col. Las Campanas, 76010 Querétaro, Querétaro, Mexico

² DIPA, PROPAC, Facultad de Química, Universidad Autónoma de Querétaro, Centro Universitario, Cerro de las Campanas s/n Col. Las Campanas, 76010 Querétaro, Querétaro, Mexico

³ Departamento de Biotecnología, Universidad Autónoma Metropolitana, Av. San Rafael Atlixco No. 186. Col. Vicentina, Iztapalapa, 09340 Mexico City, Mexico

Introduction

Lignocellulosic materials, mostly composed of lignin, cellulose, and hemicelluloses, are considered as the most abundant organic residues to be used as renewable sources for food and biofuel production [1]. Hemicellulose is a heteropolysaccharide showing xylan as a major carbohydrate component with 25–30% of the dry weight of plant cell wall [2]. Xylan is considered the second most widely available polysaccharide in nature after cellulose and can be enzymatically degraded [3]. Wide application of xylan hydrolysis into beneficial sugars, such as xylose, xylitol, and xylooligosaccharides by the enzymatic reaction of xylanase, has encouraged new efforts to improve xylan degradation efficiency [4]. Enzyme application as biocatalysts is gradually preferred over conventional chemical processes due to their high specificity and mild reaction conditions, biodegradability, and catalytic efficiency, increasing sugar yields, potentially saving costs, and making them highly competitive for industrial-scale production [5]. Nevertheless, commercial enzyme applications remain limited because of their low stability, low product recovery, and low repeated use, so the application of an immobilization technique is required [6]. Different methods, namely covalent binding, adsorption, adhesion, aggregation, entrapment, and cross-linking using diverse supports like inorganic (bentonite, ceramics, and silica) or organic materials (chitosan, alginate, polyacrylamide, agarose, cellulose, and dextrans), are available to immobilize enzymes. To date, approaches of integrating enzymes with both inorganic and organic materials, mostly comprising metal node and organic ligands as a composite, have emerged as an ideal platform for enzyme immobilization [7, 8]. In addition, integrating enzymes with composites, maintaining biological function and protecting them against denaturing conditions, mainly includes surface attachment, covalent linkage, co-precipitation, and biomimetic mineralization [9]. However, the effectiveness of each method depends on reaction conditions, product formation processing, and its cost evaluation [10]. Chitosan is characterized by being biocompatible, nontoxic, stable, sterilizable, and biodegradable. In addition, it can be prepared in a variety of forms such as powders, microparticles, and nanofibers [11, 12]. A few recent works have reported the successful immobilization of enzymes on chitosan particles leading to improved thermal and operational stability as well as safety, food, and pharmaceutical compatibility, by using the naturally occurring cross-linking agent genipin [13, 14]. Although significant efforts have been devoted to understanding the behavior of genipin as a cross-linker with chitosan in pharmaceutical and medical applications, only a few works have been devoted to exploring and correlating them with catalytic properties of enzymes [12, 14, 15]. The cross-linking technique is performed by formation of intermolecular cross-linkages of enzymes by means of bi- or multifunctional reagents. Genipin is a hydrolytic product of a geniposide extract from the fruit of *Gardenia jasminoides* Ellis. It has been proposed as a cross-linking agent because it can be up to 10,000 times less cytotoxic than conventional agents like glutaraldehyde [16]. Besides, green chemicals or natural cross-linking agents show superiority in many aspects, especially in terms of cytotoxicity [14]. On the other hand, magnetic Fe₃O₄ nanoparticles have received increasing attention in the field of immobilized enzymes due to their numerous advantages, such as simple preparation, superparamagnetism, small size, and easy separation from the reaction solution for reuse [17]. However, Fe₃O₄ magnetic nanoparticles are chemically inert; hence, they cannot be directly linked with enzymes and should be pre-coated by natural cationic macromolecules such as chitosan to obtain active functional groups for direct covalent bonding with enzymes [18]. Since xylanase also plays a crucial role in the bioconversion of hemicellulose-containing materials to monomeric sugars or xylooligosaccharides, safe

biocatalyzers and natural compounds used in their obtention process can be appreciated by food and pharmaceutical industries. The aims of this work were to produce stable enzyme complexes of cross-linked xylanase on magnetic chitosan through genipin and to evaluate its thermal properties and reusability.

Materials and Methods

Chemicals

Genipin (90% purity) was purchased from Guangxi SYBiochemical Science & Technology Co., Liuzhou, Guangxi, China. Xylanase (EC 3.2.1.8 from *Thermomyces lanuginosus*, 21.3 kDa (≥ 2500 units g^{-1})) and all chemicals were of analytical grade and purchased from Sigma-Aldrich (St. Louis, MO, USA), except those indicated.

Preparation of Magnetite Particles and Cross-Linked Magnetite–Xylanase ($Fe_3O_4@Chitosan@Xylanase$)

The magnetite particles ($Fe_3O_4@Chitosan$) were prepared by in situ co-precipitation of iron salts in a polymer template by modifying the protocol described by Morales et al. [19]. An amount of 3.6×10^{-3} mol of iron from a mixture in a molar ratio 2:1 ($Fe^{3+}:Fe^{2+}$) of ferric nitrate and ferrous sulfate was mixed at 100 rpm with 100 mg chitosan dissolved in 3% (v/v) acetic acid at 70 °C. The chitosan–iron mixture was dispersed by an ultrasonic processor (70% amplitude, VC505, Sonics & Materials, Newtown, CT, USA) for 8 min, and the generated emulsion was precipitated by adding a solution of 28% (v/v) NH_4OH :96% (v/v) ethanol in 4:1 volume ratio. The alkaline mixture was homogenized using a vortex for 30 s and then was kept under gentle shaking (60 rpm) for 18 h, followed by centrifugation for 5 min at 7000 $\times g$. The precipitate was washed with 50 mM phosphate buffer pH 7.0 and 96% (v/v) ethanol in 1:1 volume ratio, until neutralization; oven dried at 80 °C for 5 h; and ground to obtain a powder using a mortar and pestle. One gram of the powder suspended in 1 g mL^{-1} of xylanase was cross-linked with 25 mg mL^{-1} of genipin in 50 mM acetate buffer pH 4.5. The reaction was stirred for 5 min and then kept under rest for 60 min at room temperature. Then, the cross-linked magnetite–xylanase ($Fe_3O_4@Chitosan@Xylanase$) was separated from the reaction mixture by an external permanent neodymium magnet (1.2 T, Imancitos.com, Queretaro, Mexico), washed once with 70% (v/v) ethanol and then two times with Milli-Q water, and dried under vacuum at 60 °C. The immobilization yield, efficiency, and activity recovery were calculated for the $Fe_3O_4@Chitosan@Xylanase$ according to [20]. Enzyme loading (weight %) was calculated by subtracting the protein concentration that remained in the enzyme solution after immobilization from the initial protein concentration. Screening experiments evaluating the effect of the weight ratio of total iron and chitosan, sonication time over magnetic attraction, and protein loading were conducted (data not shown). The immobilized xylanase was stored at 4 °C.

Enzyme Activity Assay

The endo-1,4- β -D-xylanase activity was assayed by measuring the amount of reducing sugars (xylose equivalent) liberated from beechwood xylan (10 mg mL^{-1}) in 10 min

using 3,5-dinitrosalicylic acid (DNS) reagent, at the assay temperature [21]. The reaction was prepared according to [22] using 2.39 μM (50 mg of support per mL) and 3.75 μM of immobilized and free xylanase, respectively. At the end of the reaction, $\text{Fe}_3\text{O}_4@\text{Chitosan}@\text{Xylanase}$ nanoparticles were separated by the application of an external magnetic field and the enzymatic reaction was interrupted by the addition of the DNS reagent. Control experiments were performed with the nanoparticles but without the enzyme. One unit (U) of xylanase activity was defined as the amount of enzyme catalyzing the release of 1 μmol of reducing sugar as xylose equivalent per minute under the specified assay conditions.

Effect of Temperature and pH on endo-1,4- β -D-Xylanase Activity

To determine the optimal temperature of either free or immobilized xylanase, activity determinations were conducted by incubating at a temperature range of 30 to 90 $^\circ\text{C}$, with 10 $^\circ\text{C}$ intervals, using 50 mM citrate–phosphate buffer pH 5.0. The activation energy (E_a) and deactivation energy (E_d) of xylanase enzymes were calculated using the Arrhenius equation [23], by plotting $\ln(\text{activity})$ vs $(\text{absolute temperature, K})^{-1}$. E_a was calculated in the range of temperature where the activity rises to a maximum, and E_d was calculated in the range of temperature where the activity was lower than the maximum. The slope of this plot indicates $(-E_a R^{-1}$ and $-E_d R^{-1})$, where R is the universal gas constant. Xylanase activity was assayed at the temperature of maximum activity, using 50 mM citrate–phosphate buffer for pH values 3.0 to 7.0, 50 mM phosphate buffer for pH 8.0, and 50 mM glycine buffer for pH 9.0 and 10.0.

Kinetic Parameters of endo-1,4- β -D-Xylanase

The kinetic parameters of free and immobilized xylanase were determined by measuring the initial reaction velocity of xylanase over beechwood xylan concentrations of 0–30 mg mL^{-1} , at the optimum pH and temperature. The apparent Michaelis–Menten constant (K_m) and maximum catalytic velocity (V_{max}) values were calculated based on the Lineweaver–Burk plot method [24] for free and immobilized enzymes using the SigmaPlot 13.0 software (Systat Software, San Jose, CA, USA).

Reusability of Immobilized Xylanase

The reusability was determined by incubating the immobilized xylanase at 50, 60, and 70 $^\circ\text{C}$ at the pH of maximum activity and quantifying enzymatic activity. After the reaction, the immobilized enzyme was removed from the reaction medium, with an external permanent neodymium magnet (1.4 T), thoroughly rinsed with phosphate buffer (50 mM, pH 7.0), and then added to a fresh substrate solution to start a new enzymatic reaction cycle. The specific activity of the first reaction was set to 100%. Additionally, the separation/recollection rate of $\text{Fe}_3\text{O}_4@\text{Chitosan}@\text{Xylanase}$ after the reaction was tested. Ten milligrams of $\text{Fe}_3\text{O}_4@\text{Chitosan}@\text{Xylanase}$ was suspended in 1 mL of distilled water. The suspension of nanoparticles was mixed by vortexing for 10 s and immediately was placed in contact with a permanent neodymium magnet (1.2 T) in a range of time (3 to 15 s). The suspended solids not attracted by the magnet were removed by pipetting and the weight difference was recorded.

Characterization of Fe₃O₄@Chitosan@Xylanase

Magnetic susceptibility and magnetization studies were carried out at room temperature (20 °C) using a Microsense EV7 vibrating sample magnetometer with a maximum field of ± 18 kOe. Micrographs were taken by scanning electron (SE) microscopy in high vacuum at 15 kV using a Carl Zeiss microscope (EVO-50, Zeiss, Jena, Germany) to observe the morphology of the immobilized xylanase. A sample of Fe₃O₄@Chitosan@Xylanase dehydrated at 80 °C for 8 h was coated with gold by sputtering for 60 s and 30 mA (Desk II, Denton Vacuum, NJ, USA). The particle sizes of the magnetic support, immobilized enzyme, and chitosan were measured by dynamic light scattering (Brookhaven Instruments, Model B1-200 SM) by diluting the samples in a mixture of ethanol:water (1:1) and sonicated for 5 min. The Fourier transform-infrared spectroscopy (FT-IR) spectra were acquired from 16 scans on a Spectrum 100 infrared spectrometer (PerkinElmer, MA, USA) using 650–4000 cm⁻¹, at 1 cm⁻¹ intervals, and excluding background air. Thermogravimetric analysis (TGA) and differential scanning calorimetry (DSC) were performed by a DSC822e (Mettler-Toledo, OH, USA) equipment with a heating rate of 10 °C min⁻¹. High-purity indium was used as standard and dry nitrogen as purge gas. The thermal curves were obtained in the range 33 to 600 °C for TGA and 20 °C to 150 °C for DSC using the STARe Software (Mettler-Toledo).

Results and Discussion

Preparation of Magnetite Particles and Fe₃O₄@Chitosan@Xylanase

Xylanase was immobilized on magnetic chitosan nanoparticles via covalent bonds formed between the amino groups of chitosan and xylanase with genipin. This was a result of the formation of amide and tertiary amine mediated by complex reactions [15, 25]. *Thermomyces lanuginosus* xylanase has three Lys and eight Arg in its structure, and two Lys (119 and 144) and two Arg (145 and 161) are in the protein surface, which represent potential docking points to genipin. The immobilization yield, efficiency, and activity recovery calculated at pH 7.0 and 70 °C for the Fe₃O₄@Chitosan@Xylanase were 22.94%, 275.9%, and 63.27%, respectively. The enzyme loading was 1.0 ± 0.1 $\mu\text{g mg}^{-1}$ of magnetic support.

To the best of our knowledge, enzyme immobilization with genipin is scarcely reported. Natural cross-linking agents are currently preferred over synthetic chemicals, especially in terms of cytotoxicity when compared to traditional cross-linking reagents, such as glutaric dialdehyde, epichlorohydrin, carbodiimides, and chlorides of dicarboxylic acids [16]. Genipin is widely used for covalent cross-linking of polysaccharides featuring glucosamine units, such as chitosan, as well as proteins containing lysine and arginine [25].

Effect of Temperature and pH on endo-1,4- β -D-Xylanase Activity

The effect of temperature on relative xylanolytic activity for free and immobilized xylanase showed a similar behavior (Fig. 1a) with a 10 °C displacement in the maximum activity for immobilized xylanase. The temperature for maximum catalytic activity of free and immobilized xylanase was 60 °C and 70 °C with an activity of 64.9 $\mu\text{mol xylose (mg protein)}^{-1} \text{ min}^{-1}$ and 38.1 $\mu\text{mol xylose (mg protein)}^{-1} \text{ min}^{-1}$, respectively. A further

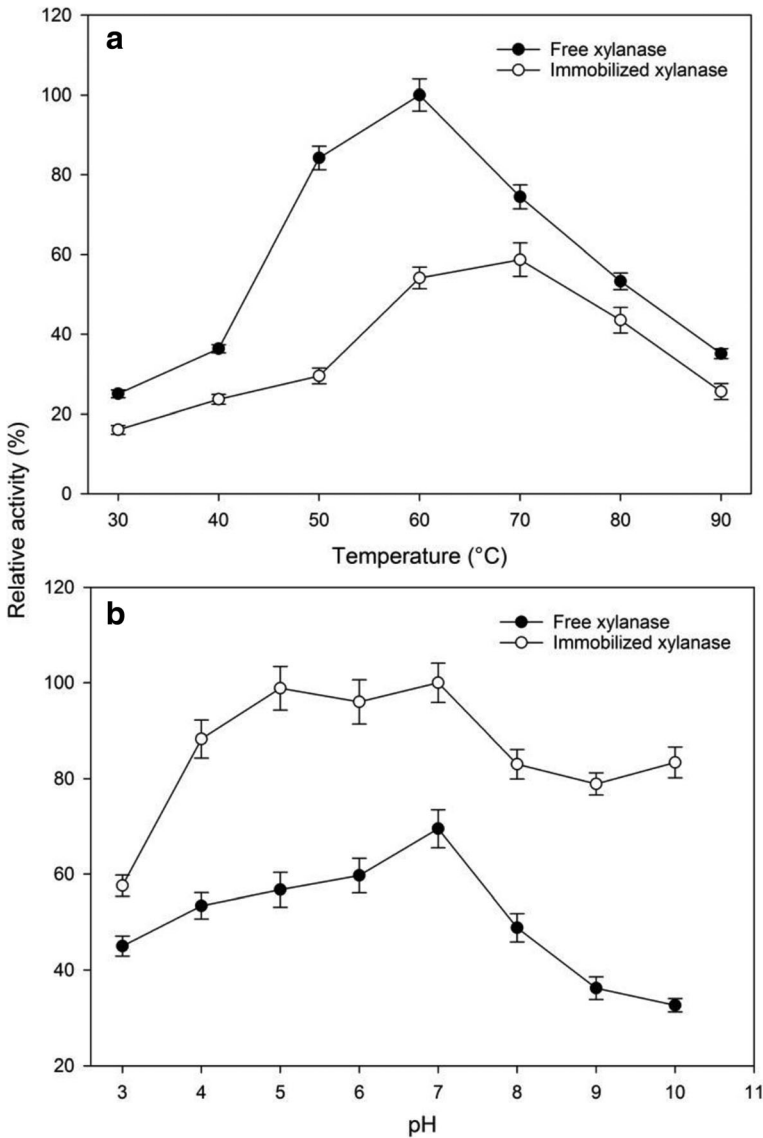


Fig. 1 Effect of temperature (a) and pH (b) on the relative activity of free and immobilized endo- β -1,4-xylanase (mean \pm SD, $n = 3$). Xylanolytic activity was determined by hydrolyzing 10 mg mL⁻¹ of beechwood xylan for 10 min

temperature rise caused a significant decrease in relative activity for the free and immobilized enzyme which might be due to conformational changes of the enzyme leading to denaturation at high temperatures. The minimal xylanolytic activity was 25.0% and 16.1% at 30 °C, whereas at 90 °C activity was 35.1% and 16.6% for free and immobilized xylanase, respectively. Following Arrhenius-type behavior, a determination coefficient (R^2) was obtained, and from the slope, the E_a and E_d were 42.0 kJ mol⁻¹ ($R^2 = 0.95$) and 29.6 kJ mol⁻¹ ($R^2 = 0.96$) and 29.1 kJ mol⁻¹ ($R^2 = 0.99$) and 33.7 kJ mol⁻¹ ($R^2 = 0.97$) for free and immobilized xylanase,

respectively. Thus, more energy is required to start the xylanolytic activity and less energy to stop the xylanolytic activity in the free enzyme when compared to the immobilized enzyme. The temperature of maximum activity for free xylanase used in this study of *T. lanuginosus* is in agreement with those previously reported [26–28]. It was evident that the immobilization protocol used in this work successfully increased protein thermal stability, and could be important for application of $\text{Fe}_3\text{O}_4@\text{Chitosan}@\text{Xylanase}$ in the harsh temperature condition of relevant industries.

In relation to the effect of pH activity, the immobilized xylanase showed more stability at pH variations (4 to 7) in the reaction medium, opposite to free xylanase activity (Fig. 1b). A maximum enzymatic activity of $38.1 \mu\text{mol xylose (mg protein)}^{-1} \text{ min}^{-1}$ and $64.9 \mu\text{mol xylose (mg protein)}^{-1} \text{ min}^{-1}$ was observed at pH 7.0 for the free and immobilized xylanase, respectively. The activity of free xylanase decreased as the pH changed from 7.0, exhibiting the common bell shape. The immobilized enzyme retained about 10% more activity than the free xylanase in the pH range of 4.0 to 6.0. These results suggest that cross-linking onto the magnetic support provided a shelter to xylanase at acid pH, associated to alterations in the general physical nature of the enzyme. Xylanolytic activity for $\text{Fe}_3\text{O}_4@\text{Chitosan}@\text{Xylanase}$ was 80% of the maximum in the pH range of 8.0 to 10.0, whereas in this pH range, free xylanase only showed from 70 to 50% of its maximum activity. Thus, enzymatic activity can be well retained when xylanase is cross-linked to the magnetic support and should be considered in practical issues. Reviews about the immobilization of different enzymes suggest that the effect of temperature and pH on the catalytic behavior of an enzyme varies with the type of matrix and immobilization method used [29–31].

The enhanced thermal and pH stability showed by $\text{Fe}_3\text{O}_4@\text{Chitosan}@\text{Xylanase}$ is probably due to a large number of interactions between the magnetic composite and xylanase. These interactions may provide a more rigid external backbone for enzyme binding and proper hydrophilic/hydrophobic balance and surface chemistry [31]. Thus, the effect of high temperature or extreme pH values on the removal of interactions or unfolding of the secondary/tertiary structures of enzymes is minimized [30]. In addition, in polyionic matrices such as chitosan, a partitioning effect of protons between the bulk phase and the enzyme microenvironment during the hydrolysis has been reported, causing less effect to catalysis by the acidic conditions [18]. Additional studies are needed to validate this hypothesis.

Kinetic Parameters of endo-1,4- β -D-Xylanase

The apparent Michaelis–Menten constants (K_m) and maximum activity (V_{max}) of free and $\text{Fe}_3\text{O}_4@\text{Chitosan}@\text{Xylanase}$ were 19.06 mg mL^{-1} and $8.07 \mu\text{mol min}^{-1} \text{ mL}^{-1}$, and 4.26 mg mL^{-1} and $10.34 \mu\text{mol min}^{-1} \text{ mL}^{-1}$, respectively (Fig. 2). The K_m for xylanase activity of $\text{Fe}_3\text{O}_4@\text{Chitosan}@\text{Xylanase}$ was 4.47 times lower than that of the free enzyme, whereas the V_{max} of the nanoparticles was 0.28 times higher than that of the free enzyme. Generally, enzyme immobilization negatively affects both K_m and V_{max} values, compared to the free enzymes, mainly due to external and substrate diffusion limitations, steric hindrance of the active site by the support or loss of enzyme flexibility necessary for substrate binding [32, 33]. In this work, a low K_m suggested strong enzyme–substrate affinity, so the best stabilization of the transition state resulted when the substrate bound to the active site of the immobilized enzyme than of the free enzyme. Besides, the decrease in K_m value is likely to occur due to the fact that the local concentration of the negative charge of the substrate increases because of the positively charged matrix near the immobilized enzyme [34]. On the

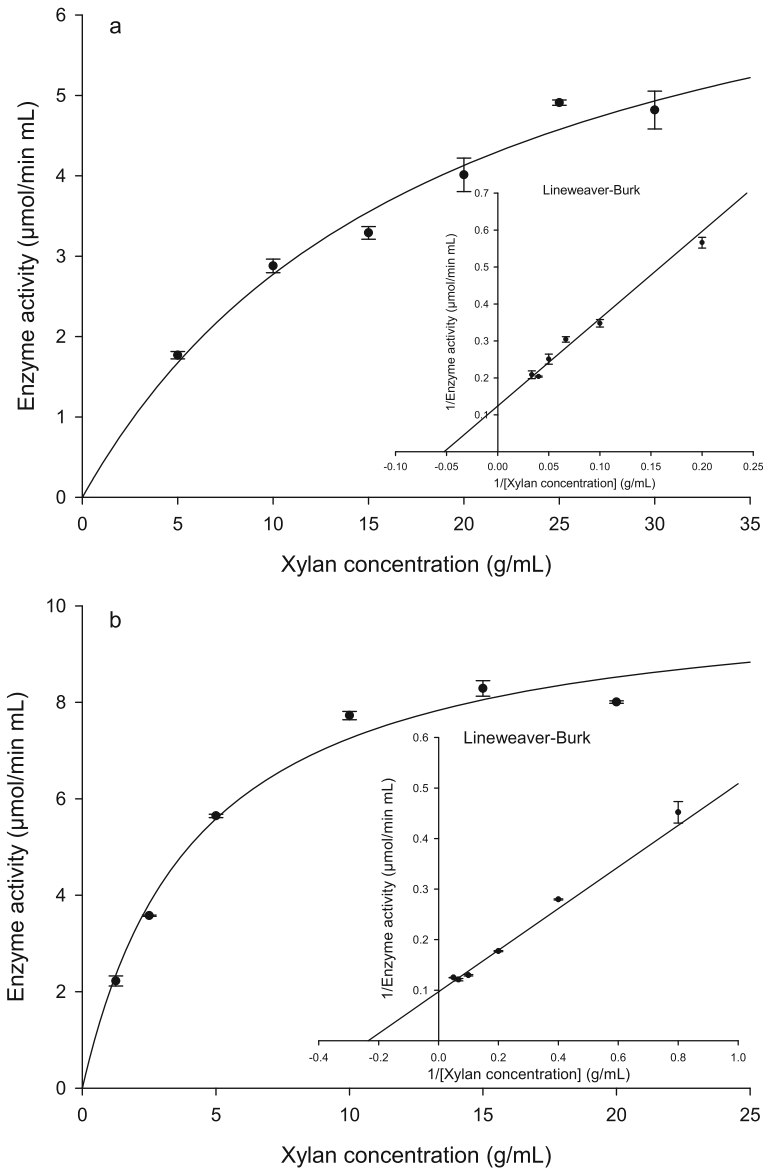


Fig. 2 Michaelis–Menten curves for the free (a) and immobilized (b) xylanase. Inset: The Hanes–Wolf plots of free (a) and immobilized (b) xylanase for calculating kinetic parameters

other hand, the increase in V_{max} indicates a higher efficiency of the immobilized enzyme. These results were in agreement with the immobilization efficiency value.

Reusability of Immobilized Xylanase

The $Fe_3O_4@Chitosan@Xylanase$ was reused for three successive cycles retaining 50% of its initial activity when incubated at 70 °C (Fig. 3). Additionally, 78% and 69% loss in initial

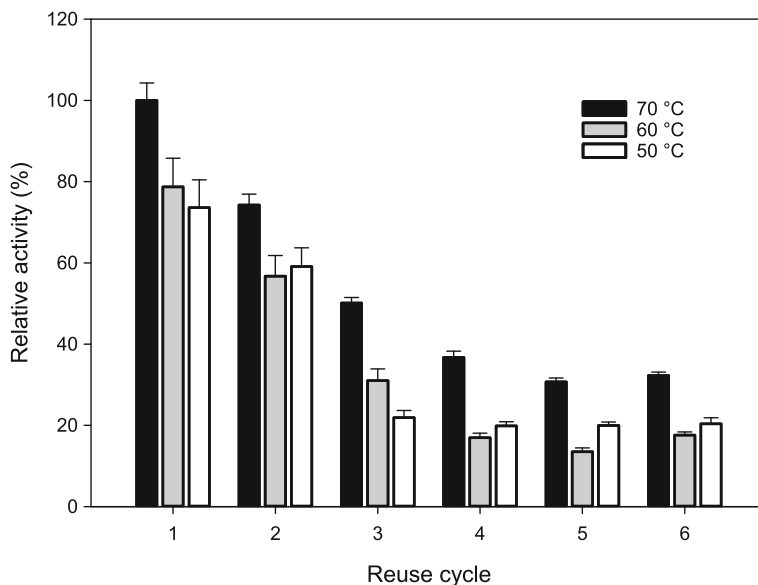


Fig. 3 Reusability of Fe_3O_4 @Chitosan@Xylanase over six consecutive cycles incubated at 70 °C, 60 °C, and 50 °C with phosphate buffer (50 mM, pH 7.0) (mean \pm SD, $n = 3$). The immobilized xylanase was incubated again with a fresh substrate to initiate the next cycle of hydrolysis. Each hydrolysis cycle lasted 10 min

activity was observed in the third cycle when incubated at 60 and 50 °C, respectively, suggesting better stability at higher temperatures. The maximum separation/recollection rate of Fe_3O_4 @Chitosan@Xylanase recorded after the reaction was 2.06 mg of support per second in the first 3 s, which represents more than 50% of the mass attracted by the magnet. From 5 to 15 s, the separation/recollection rate decelerated to half of the maximum rate. Activity losses have been attributed to enzyme inactivation during repeated recycling, despite the fact that immobilization processes have been developed to improve enzyme stability [35, 36]. The reusability of the immobilized enzyme is a key factor for practical applications to reduce cost and simplify the processes.

Characterization of Fe_3O_4 @Chitosan@Xylanase

The saturation magnetization (M_s) of the Fe_3O_4 , Fe_3O_4 @Chitosan and Fe_3O_4 @Chitosan@Xylanase particles was 54.1 emu (g of sample) $^{-1}$, 41.9 emu (g of sample) $^{-1}$, and 33.89 emu (g of sample) $^{-1}$, respectively. There was a scarce remanent magnetization of 0.7186 emu (g of sample) $^{-1}$, 0.3197 emu (g of sample) $^{-1}$, and 0.1919 emu (g of sample) $^{-1}$ and a small coercive field of 12.8 Oe, 3.61 Oe, and 6.16 Oe for Fe_3O_4 , Fe_3O_4 @Chitosan, and Fe_3O_4 @Chitosan@Xylanase particles, respectively. These data in addition to the magnetization curve indicated the existence of superparamagnetism in the nanoparticles (Fig. 4). A wide range of M_s values 98–30 emu (g of sample) $^{-1}$ was reported for uncoated and coated Fe_3O_4 particles which depend on the synthesis method and nature of the coating [37, 38]. Thus, values of M_s around 30 emu (g of sample) $^{-1}$ indicated the presence of nonmagnetic polymer coating on the surface of magnetic iron oxide [39]. The magnetic particles preferentially should be superparamagnetic so that they are magnetic only under an external magnetic field and then become inactive once the magnetic field is removed [40].

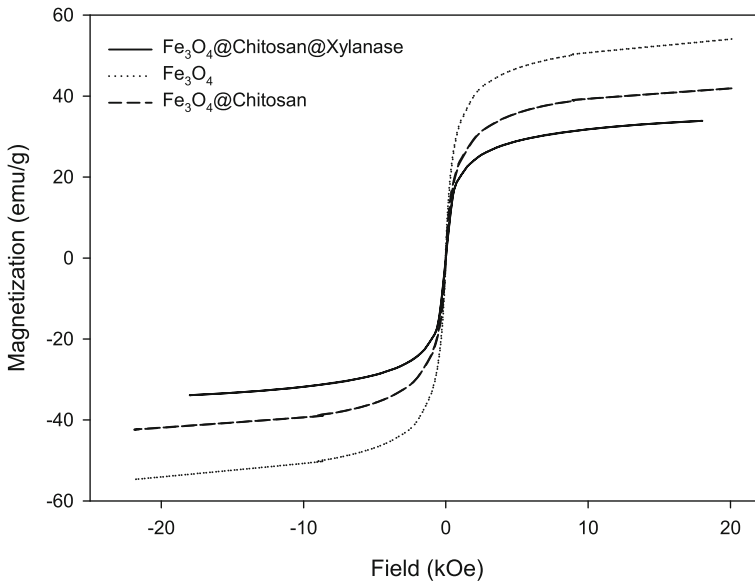


Fig. 4 Magnetization curve of $\text{Fe}_3\text{O}_4@Chitosan@Xylanase$

Recently, magnetite nanoparticles have been used for the preparation of immobilized enzymes, which can be easily separated using magnetic fields, thereby eliminating the need for filtration and centrifugation techniques [41].

Micrographs of $\text{Fe}_3\text{O}_4@Chitosan@Xylanase$ were taken to obtain information on their morphology. Figure 5 shows different magnifications of mainly defined shapes of particles with a wide range in size forming heterogeneous aggregates. The particle size of $\text{Fe}_3\text{O}_4@Chitosan$, $\text{Fe}_3\text{O}_4@Chitosan@Xylanase$, and chitosan was determined by dynamic light scattering. The histograms of $\text{Fe}_3\text{O}_4@Chitosan$ showed a narrow particle size distribution with an average of 32.5 nm contrasting with the $\text{Fe}_3\text{O}_4@Chitosan@Xylanase$ which showed a bimodal histogram, with two different particle distributions and with an average particle size of 254 nm. This can be attributed to the fact that the particles form aggregates as shown in the SE micrographs. Finally, the chitosan shows a wider distribution (200 to 800 nm), with an average particle size of 395.5 nm.

The FT-IR spectra (Fig. 6) reveal characteristic bands of the chemical groups found in xylanase, $\text{Fe}_3\text{O}_4@Chitosan$, and $\text{Fe}_3\text{O}_4@Chitosan@Xylanase$. The spectra of xylanase showed signals around 3200 and 3400 cm^{-1} , corresponding to C–H and OH bonds as well as the NH stretching. Also, the characteristic bands at approximately 1650 and 1540 cm^{-1} were assigned to vibration of the amide I (C=O) and II (N–H), present in the protein backbone. Signals between 950 and 1150 cm^{-1} can be assigned to C–C, C–O, and C–N bonds which were present in xylanase and chitosan. Signals around 650 cm^{-1} identified as Fe–O bonds, characteristic of magnetite, were observed in all spectra. Peaks between 1350 and 1650 cm^{-1} are related to the stretching vibrations of the amide (OC–NH) bonds present in both chitosan and xylanase. The structural change in FT-IR spectra confirmed the successful cross-linking of the xylanase to the $\text{Fe}_3\text{O}_4@Chitosan$ via formation of amide bonds between carboxyl and amino groups. These descriptive results agree with the literature [38, 42, 43].

The free enzyme, magnetic support, and immobilized enzyme were subjected to a thermal analysis technique that allows measuring weight loss and energy changes in the temperature

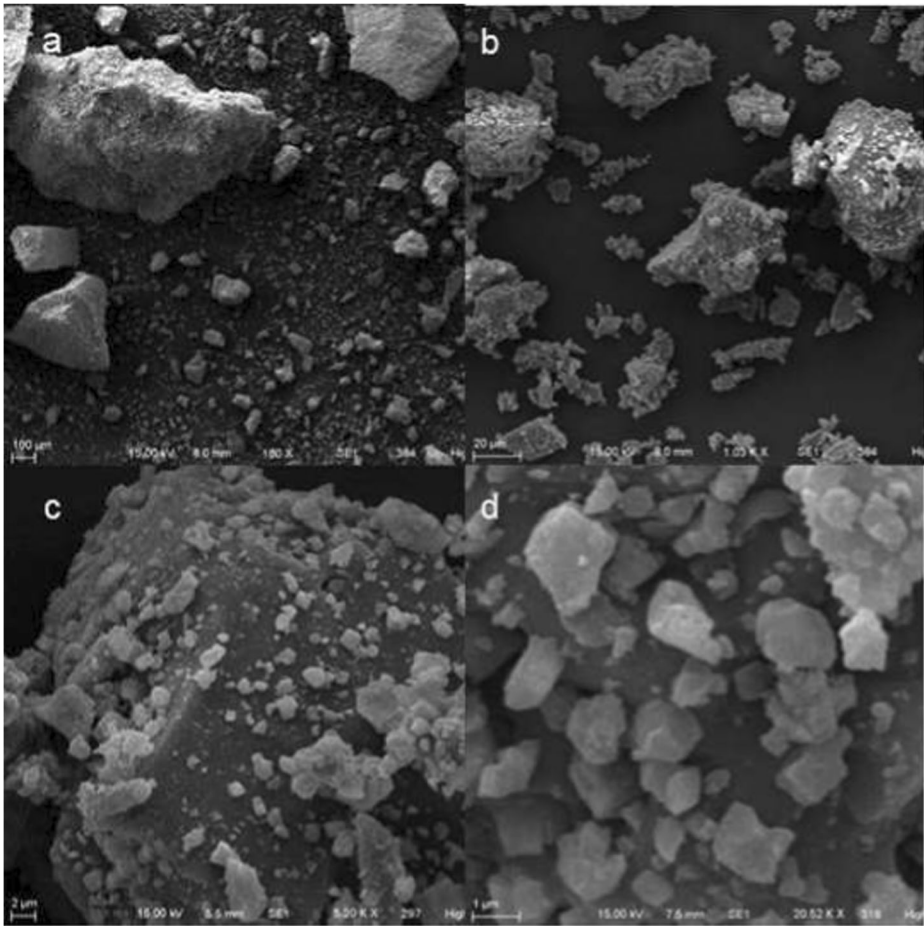


Fig. 5 SE micrographs of $\text{Fe}_3\text{O}_4@Chitosan@Xylanase$ at $\times 100$ (a), $\times 1000$ (b), $\times 5000$ (c), and $\times 20,000$ (d)

range of 33 to 600 °C. However, the effect of the energy on the enzyme was significant up to 100 °C (Fig. 7). The thermogram profiles of free xylanase and $\text{Fe}_3\text{O}_4@Chitosan@Xylanase$ show similar weight loss behavior, of approximately 15% and 10%, respectively, at temperatures ranging from 33 to 190 °C. In contrast, weight loss of 7% was observed for $\text{Fe}_3\text{O}_4@Chitosan$. The weight loss in this range of temperatures is mainly due to the loss of low molecular mass compounds and adsorbed and partly bound water. From 250 to 350 °C, a rapid weight loss down to 36% in free xylanase is shown. In contrast, the weight lost for $\text{Fe}_3\text{O}_4@Chitosan$ and $\text{Fe}_3\text{O}_4@Chitosan@Xylanase$ was 25%. This behavior corresponds to the degradation of the chitosan, genipin, proteins, and structurally bound water. The complete degradation of organic compounds is shown from 350 to 600 °C. Among the samples, the free xylanase was more susceptible to the effect of applied energy. Moreover, free xylanase and $\text{Fe}_3\text{O}_4@Chitosan@Xylanase$ thermograms show the first shift in weight loss profile at 67 °C and 97 °C, respectively. Furthermore, a structural change can be observed at approximately 62 and 63 °C for the free and immobilized enzyme, respectively, in DSC profiles. These inflection points were consistent with the optimal temperature of the free and immobilized enzyme. The broad endotherms are indicative of polydispersity of the molecular interactions, consistent with

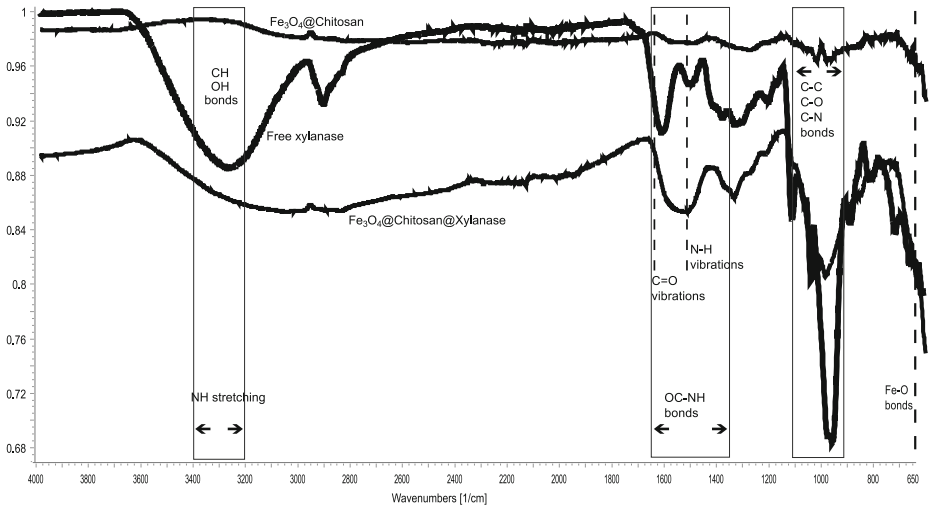


Fig. 6 FT-IR spectra of the Fe_3O_4 @Chitosan, free xylanase, and Fe_3O_4 @Chitosan@Xylanase

dynamic light scattering observations. The apparent melting temperature (T_m) related to the first structural change in the samples could be calculated and compared given the irreversibility of denaturation in the free and immobilized xylanase. The melting point was around 63°C for free xylanase and Fe_3O_4 @Chitosan@Xylanase. In the case of magnetic support, the first structural change was observed at approximately 75°C . Additionally, the immobilized enzyme requires 1.4 times more energy to present the first structural change compared to the free enzyme. These results were in agreement with that of other authors [30, 32] who demonstrated that the cross-linking of enzymes to a support provides thermal protection for a longer time and further enhanced the thermal stability of the immobilized enzyme. Besides, other authors [4, 31, 44] have demonstrated that cross-linking can provide a more effective conformational

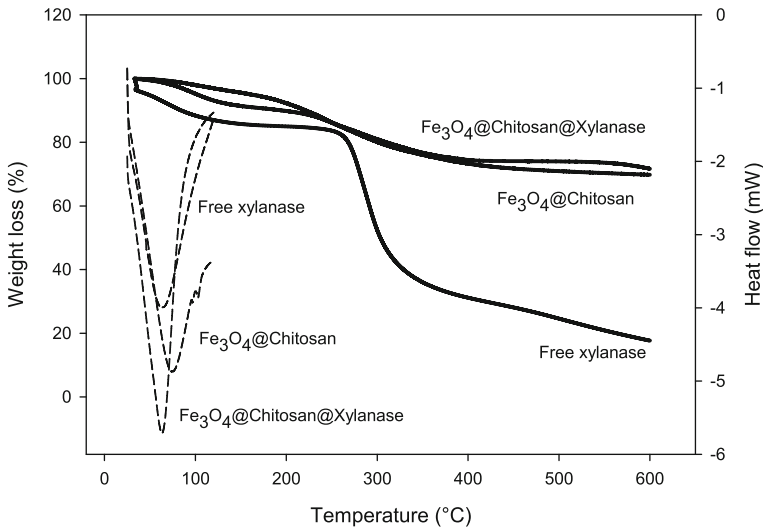


Fig. 7 Thermogravimetric and differential scanning calorimetry profiles of free xylanase, Fe_3O_4 @Chitosan@Xylanase, and Fe_3O_4 @Chitosan

stabilization of enzymes due to the rigidity of the structure making it to require more energy to break down. The multipoint attachment of the immobilized enzyme molecules prevented enzyme denaturation compared to the free enzyme.

Conclusion

Fe₃O₄@Chitosan was successfully prepared by alkaline co-precipitation and was cross-linked to a xylanase using genipin. The synthesized Fe₃O₄@Chitosan@Xylanase using natural compounds could be attractive to produce xylooligosaccharides with food and pharmaceutical applications. The immobilized xylanase could be recycled by extraction from the reactor using magnetism and exhibited improved stability during thermal and pH treatments. Cross-linking mediated by genipin can provide a more effective conformational stabilization of enzymes, and more energy is required to break down this active conformation compared to free enzymes. A process involving biocatalyzers which can be simply and rapidly separated from the reaction solution by an ordinary magnet can be economical and feasible.

Acknowledgments This work was supported by the Consejo Nacional de Ciencia y Tecnología, Mexico [CB-2014-241208].

Compliance with Ethical Standards

Conflict of Interest The authors declare that they have no conflict of interest.

References

1. Sorek, N., Yeats, T. H., Szemenyei, H., Youngs, H., & Somerville, C. R. (2014). The implications of lignocellulosic biomass chemical composition for the production of advanced biofuels. *BioScience*, *64*(3), 192–201. <https://doi.org/10.1093/biosci/bit037>.
2. Saka, S., & Bae, H. J. (2016). Secondary xylem for bioconversion. In K. Yoon soo, F. Ryo, & P. S. Adya (Eds.), *Secondary xylem biology: origins, functions, and applications* (pp. 213–231). Academic Press. <https://doi.org/10.1016/B978-0-12-802185-9.00011-5>.
3. Dutta, S. K., & Chakraborty, S. (2015). Kinetic analysis of two-phase enzymatic hydrolysis of hemicellulose of xylan type. *Bioresource Technology*, *198*, 642–650. <https://doi.org/10.1016/j.biortech.2015.09.066>.
4. Sukri, S. S. M., & Munaim, M. S. A. (2017). Combination of entrapment and covalent binding techniques for xylanase immobilisation on alginate beads: screening process parameters. *Chemical Engineering Transactions*, *56*, 169–174. <https://doi.org/10.3303/CET1756029>.
5. Bibi, Z., Ansari, A., Zohra, R. R., Aman, A., & Ul Qader, S. A. (2014). Production of xylan degrading endo-1, 4-β-xylanase from thermophilic *Geobacillus stearothermophilus* KIBGE-IB29. *Journal of Radiation Research and Applied Sciences*, *7*(4), 478–485. <https://doi.org/10.1016/j.jrras.2014.08.001>.
6. Bhushan, B., Pal, A., & Jain, V. (2015). Improved enzyme catalytic characteristics upon glutaraldehyde cross-linking of alginate entrapped xylanase isolated from *Aspergillus flavus* MTCC 9390. *Enzyme Research*, *2015*, 1–9. <https://doi.org/10.1155/2015/210784>.
7. Lyu, F., Zhang, Y., Zare, R. N., Ge, J., & Liu, Z. (2014). One-pot synthesis of protein-embedded metal-organic frameworks with enhanced biological activities. *Nano Letters*, *14*(10), 5761–5765. <https://doi.org/10.1021/nl5026419>.
8. Li, Z., Xia, H., Li, S., Pang, J., Zhu, W., & Jiang, Y. (2017). In situ hybridization of enzymes and their metal-organic framework analogues with enhanced activity and stability by biomimetic mineralisation. *Nanoscale*, *9*(40), 15298–15302. <https://doi.org/10.1039/c7nr06315f>.

9. Xia, H., Zhong, X., Li, Z., & Jiang, Y. (2019). Palladium-mediated hybrid biocatalysts with enhanced enzymatic catalytic performance via allosteric effects. *Journal of Colloid and Interface Science*, 533, 1–8. <https://doi.org/10.1016/j.jcis.2018.08.052>.
10. Romo Sánchez, S., Gil Sánchez, I., Arévalo-Villena, M., & Briones Pérez, A. (2015). Production and immobilization of enzymes by solid-state fermentation of agroindustrial waste. *Bioprocess and Biosystems Engineering*, 38(3), 587–593. <https://doi.org/10.1007/s00449-014-1298-y>.
11. Kaur, S., & Dhillon, G. S. (2014). The versatile biopolymer chitosan: potential sources, evaluation of extraction methods and applications. *Critical Reviews in Microbiology*, 40(2), 155–175. <https://doi.org/10.3109/1040841X.2013.770385>.
12. Manickam, B., Sreedharan, R., & Elumalai, M. (2014). “Genipin”—the natural water soluble cross-linking agent and its importance in the modified drug delivery systems: an overview. *Current Drug Delivery*, 11(1), 139–145. <https://doi.org/10.2174/15672018113106660059>.
13. Klein, M. P., Hackenhaar, C. R., Lorenzoni, A. S. G., Rodrigues, R. C., Costa, T. M. H., Ninow, J. L., & Hertz, P. F. (2016). Chitosan crosslinked with genipin as support matrix for application in food process: support characterization and β -D-galactosidase immobilization. *Carbohydrate Polymers*, 137, 184–190. <https://doi.org/10.1016/j.carbpol.2015.10.069>.
14. Lau, Y. T., Kwok, L. F., Tam, K. W., Chan, Y. S., Shum, D. K. Y., & Shea, G. K. H. (2018). Genipin-treated chitosan nanofibers as a novel scaffold for nerve guidance channel design. *Colloids and Surfaces B: Biointerfaces*, 162, 126–134. <https://doi.org/10.1016/j.colsurfb.2017.11.061>.
15. Pozzo L., d. Y., da Conceição, T. F., Spinelli, A., Scharnagl, N., & Pires, A. T. N. (2018). Chitosan coatings crosslinked with genipin for corrosion protection of AZ31 magnesium alloy sheets. *Carbohydrate Polymers*, 181(September 2017), 71–77. <https://doi.org/10.1016/j.carbpol.2017.10.055>.
16. Oryan, A., Kamali, A., Moshiri, A., Baharvand, H., & Daemi, H. (2018). Chemical crosslinking of biopolymeric scaffolds: current knowledge and future directions of crosslinked engineered bone scaffolds. *International Journal of Biological Macromolecules*, 107(PartA), 678–688. <https://doi.org/10.1016/j.ijbiomac.2017.08.184>.
17. Feng, J., Yu, S., Li, J., Mo, T., & Li, P. (2016). Enhancement of the catalytic activity and stability of immobilized aminoacylase using modified magnetic Fe₃O₄ nanoparticles. *Chemical Engineering Journal*, 286, 216–222. <https://doi.org/10.1016/j.cej.2015.10.083>.
18. Liu, M. Q., Dai, X. J., Guan, R. F., & Xu, X. (2014). Immobilization of *Aspergillus niger* xylanase A on Fe₃O₄-coated chitosan magnetic nanoparticles for xylooligosaccharide preparation. *Catalysis Communications*, 55, 6–10. <https://doi.org/10.1016/j.catcom.2014.06.002>.
19. Morales, M. A., De Souza Rodrigues, E. C., De Amorim, A. S. C. M., Soares, J. M., & Galembeck, F. (2013). Size selected synthesis of magnetite nanoparticles in chitosan matrix. *Applied Surface Science*, 275, 71–74. <https://doi.org/10.1016/j.apsusc.2013.01.123>.
20. Sheldon, R. A., & Van Pelt, S. (2013). Enzyme immobilisation in biocatalysis: why, what and how. *Chemical Society Reviews*, 42(42), 6223–6235. <https://doi.org/10.1039/c3cs60075k>.
21. Miller, G. L. (1959). Use of dinitrosalicylic acid reagent for determination of reducing sugar. *Analytical Chemistry*, 31(3), 426–428. <https://doi.org/10.1021/ac60147a030>.
22. Length, F. (2011). Homologue expression of a fungal endo-1, 4- -D- xylanase using submerged and solid substrate fermentations. *Journal of Biotechnology*, 10(10), 1760–1767. <https://doi.org/10.5897/AJB10.1952>.
23. Goluguri, B. R., Thulluri, C., Addepally, U., & Shetty, P. R. (2016). Novel alkali-thermostable xylanase from *Thielaviopsis basicola* (MTCC 1467): purification and kinetic characterization. *International Journal of Biological Macromolecules*, 82, 823–829. <https://doi.org/10.1016/j.ijbiomac.2015.10.055>.
24. Lineweaver, H., & Burk, D. (1934). The determination of enzyme dissociation constants. *Journal of the American Chemical Society*, 56(3), 658–666. <https://doi.org/10.1021/ja01318a036>.
25. Tokareva, M. I., Ivantsova, M. N., & Mironov, M. A. (2017). Heterocycles of natural origin as non-toxic reagents for cross-linking of proteins and polysaccharides. *Chemistry of Heterocyclic Compounds*, 53(1), 21–35. <https://doi.org/10.1007/s10593-017-2016-x>.
26. Mehnaati-Najafabadi, V., Taheri-Kafrani, A., & Bordbar, A.-K. (2017). Xylanase immobilization on modified superparamagnetic graphene oxide nanocomposite: effect of PEGylation on activity and stability. *International Journal of Biological Macromolecules*, 107(Pt A), 418–425. <https://doi.org/10.1016/j.ijbiomac.2017.09.013>.
27. Shahrestani, H., Taheri-Kafrani, A., Soozanipour, A., & Tavakoli, O. (2016). Enzymatic clarification of fruit juices using xylanase immobilized on 1,3,5-triazine-functionalized silica-encapsulated magnetic nanoparticles. *Biochemical Engineering Journal*, 109, 51–58. <https://doi.org/10.1016/j.bej.2015.12.013>.
28. Soozanipour, A., Taheri-Kafrani, A., & Landarani Isfahani, A. (2015). Covalent attachment of xylanase on functionalized magnetic nanoparticles and determination of its activity and stability. *Chemical Engineering Journal*, 270, 235–243. <https://doi.org/10.1016/j.cej.2015.02.032>.

29. Selvarajan, E., & Veena, R. (2017). Recent advances and future perspectives of thermostable xylanase. *Biomedical & Pharmacology Journal*, *10*(1), 261–279. <https://doi.org/10.13005/bpj/1106>.
30. Vaz, R. P., de Souza Moreira, L. R., & Ferreira Filho, E. X. (2016). An overview of holocellulose-degrading enzyme immobilization for use in bioethanol production. *Journal of Molecular Catalysis B: Enzymatic*, *133*, 127–135. <https://doi.org/10.1016/j.molcatb.2016.08.006>.
31. Mohamad, N. R., Marzuki, N. H. C., Buang, N. A., Huyop, F., & Wahab, R. A. (2015). An overview of technologies for immobilization of enzymes and surface analysis techniques for immobilized enzymes. *Biotechnology and Biotechnological Equipment*, *29*(2), 205–220. <https://doi.org/10.1080/13102818.2015.1008192>.
32. Kumar, S., Haq, I., Prakash, J., & Raj, A. (2017). Improved enzyme properties upon glutaraldehyde cross-linking of alginate entrapped xylanase from *Bacillus licheniformis*. *International Journal of Biological Macromolecules*, *98*, 24–33. <https://doi.org/10.1016/j.ijbiomac.2017.01.104>.
33. Liu, M. Q., Huo, W. K., Xu, X., & Jin, D. F. (2015). An immobilized bifunctional xylanase on carbon-coated chitosan nanoparticles with a potential application in xylan-rich biomass bioconversion. *Journal of Molecular Catalysis B: Enzymatic*, *120*, 119–126. <https://doi.org/10.1016/j.molcatb.2015.07.002>.
34. Hou, L., Sun, X., Sui, J., & Ding, C. (2015). Immobilization of a 22kDa xylanase on Eudragit L-100 for xylo-oligosaccharide production. *Advance Journal of Food Science and Technology*, *7*(6), 401–407. <https://doi.org/10.19026/ajfst.7.1332>.
35. Bagewadi, Z. K., Mulla, S. I., Shouche, Y., & Ninnekar, H. Z. (2016). Xylanase production from *Penicillium citrinum* isolate HZN13 using response surface methodology and characterization of immobilized xylanase on glutaraldehyde-activated calcium-alginate beads. *3 Biotech*, *6*(2), 1–18. <https://doi.org/10.1007/s13205-016-0484-9>.
36. Chen, J., Leng, J., Yang, X., Liao, L., Liu, L., & Xiao, A. (2017). Enhanced performance of magnetic graphene oxide-immobilized laccase and its application for the decolorization of dyes. *Molecules*, *22*(2), 221. <https://doi.org/10.3390/molecules22020221>.
37. Al-Qodah, Z., Al-Shannag, M., Al-Busoul, M., Penchev, I., & Orfali, W. (2017). Immobilized enzymes bioreactors utilizing a magnetic field: a review. *Biochemical Engineering Journal*, *121*, 94–106. <https://doi.org/10.1016/j.bej.2017.02.003>.
38. Pati, S. S., Singh, L. H., Guimaraes, E. M., Mantilla, J., Coaquira, J. A. H., Oliveira, A. C., et al. (2016). Magnetic chitosan-functionalized Fe₃O₄@Au nanoparticles: synthesis and characterization. *Journal of Alloys and Compounds*, *684*, 68–74. <https://doi.org/10.1016/j.jallcom.2016.05.160>.
39. Prabha, G., & Raj, V. (2016). Preparation and characterization of chitosan-polyethylene glycol-polyvinylpyrrolidone-coated superparamagnetic iron oxide nanoparticles as carrier system: drug loading and in vitro drug release study. *Journal of Biomedical Materials Research - Part B Applied Biomaterials*, *104*(4), 808–816. <https://doi.org/10.1002/jbm.b.33637>.
40. Saikia, C., Das, M. K., Ramteke, A., & Maji, T. K. (2016). Effect of crosslinker on drug delivery properties of curcumin loaded starch coated iron oxide nanoparticles. *International Journal of Biological Macromolecules*, *93*(Pt A), 1121–1132. <https://doi.org/10.1016/j.ijbiomac.2016.09.043>.
41. Bhattacharya, A., & Pletschke, B. I. (2014). Magnetic cross-linked enzyme aggregates (CLEAs): a novel concept towards carrier free immobilization of lignocellulolytic enzymes. *Enzyme and Microbial Technology*, *61–62*, 17–27. <https://doi.org/10.1016/j.enzmictec.2014.04.009>.
42. Jia, L., Budinova, G. A. L. G., Takasugi, Y., Noda, S., Tanaka, T., Ichinose, H., Goto, M., & Kamiya, N. (2016). Synergistic degradation of arabinoxylan by free and immobilized xylanases and arabinofuranosidase. *Biochemical Engineering Journal*, *114*, 268–275. <https://doi.org/10.1016/j.bej.2016.07.013>.
43. Waifalkar, P. P., Parit, S. B., Chougale, A. D., Sahoo, S. C., Patil, P. S., & Patil, P. B. (2016). Immobilization of invertase on chitosan coated γ -Fe₂O₃ magnetic nanoparticles to facilitate magnetic separation. *Journal of Colloid and Interface Science*, *482*, 159–164. <https://doi.org/10.1016/j.jcis.2016.07.082>.
44. Li, L., Li, G., Cao, L. C., Ren, G. H., Kong, W., Di Wang, S., et al. (2015). Characterization of the cross-linked enzyme aggregates of a novel β -galactosidase, a potential catalyst for the synthesis of galacto-oligosaccharides. *Journal of Agricultural and Food Chemistry*, *63*(3), 894–901. <https://doi.org/10.1021/jf504473k>.